P9.6 ECHO CLASSIFICATION WITHIN THE SPECTRAL DOMAIN TO DISCRIMINATE GROUND CLUTTER FROM METEOROLOGICAL TARGETS

Mike Dixon, Cathy Kessinger and John Hubbert
National Center for Atmospheric Research*, Boulder, Colorado

Abstract: Clutter filters tend to remove meteorological signals in situations in which the spectral signature of the weather (especially stratiform precipitation) resembles that of ground clutter. To better discriminate between weather and ground clutter additional information is required. Promising sources of such information are (a) the nature of the reflectivity pattern around the clutter target, (b) the variance of the velocity, (c) spectral characteristics, and (d) the variance of dual polarization variables. We present a radar echo classification scheme based on a fuzzy combination of these variables. We apply this scheme to a case and demonstrate that it is effective in discriminating between ground clutter and weather echoes. This classification scheme is suitable for real-time radar applications and can be used as a decision support system to control the application of the clutter filters to only clutter targets and not to weather echoes. Better preservation of the reflectivity values within stratiform precipitation that is near the zero ms^{-1} radial velocity contour is achieved.

1 Introduction

Radar ground clutter, both NP (normal propagation) and AP (anomalous propagation), complicate the interpretation of weather targets. An ideal clutter filtering system will remove the clutter power while not altering the weather power. In practice, filters do this with varying degrees of success.

One particular challenge arises from the fact that in some situations (for example stratiform precipitation with radial velocity close to zero and a narrow spectrum width) weather and clutter spectra have very similar characteristics, making it difficult to distinguish one from the other. In this paper, we present a methodology for dealing with this challenge.

Corresponding author: Cathy Kessinger, NCAR/RAP, P.O. Box 3000, Boulder, CO 80307 email: kessinger@ucar.edu

First, we discuss a spectral clutter filter. The width and depth of the clutter filter is determined by the characteristics of the spectrum to be filtered and thus the clutter filter is adaptive. We can obtain considerable information about the clutter and weather at a gate by considering only the characteristics of a single spectrum.

In the second part of the paper, we will present techniques to resolve the ambiguity that sometimes occurs when trying to distinguish clutter from weather. In order to distinguish zero velocity weather from ground clutter, more information is required. This can come from two possible sources: (a) the spectra at gates surrounding the gate of interest (using fuzzy logic techniques – see later) and (b) dual-polarization fields, if they are available.

2 Interpreting weather and clutter signatures in spectra from Doppler radars

The receiver in a Doppler radar measures returns in the form of voltages which represent complex numbers, I (real) and Q (imaginary), with Q lagging I by 90 degrees (a quarter wavelength). The raw I/Q pairs are considered to be in the ‘time domain’, since they represent returns from a series of pulses in time.

The time-domain I/Q data may be transformed into the ‘spectral domain’ or ‘frequency domain’ via the application of a 1-dimensional complex Fourier transform which yields the frequency or velocity spectrum. This transformation is a technique for analyzing the movement of the scatterers relative to the radar.

Figure 1 shows an example of a 64-point spectrum containing power from both clutter and weather. (This simulated spectrum is reconstructed from clutter and weather components). The red line shows the weather spectrum, the green line shows the clutter spectrum and the blue line shows the combined spectrum. The radial velocity is plotted on the X axis and the power at each sample point is plotted on the Y axis using a log scale. The zero-velocity point is plotted at the center of the X axis, with motion away from the radar plotted on the right side and motion towards the radar on the left side.

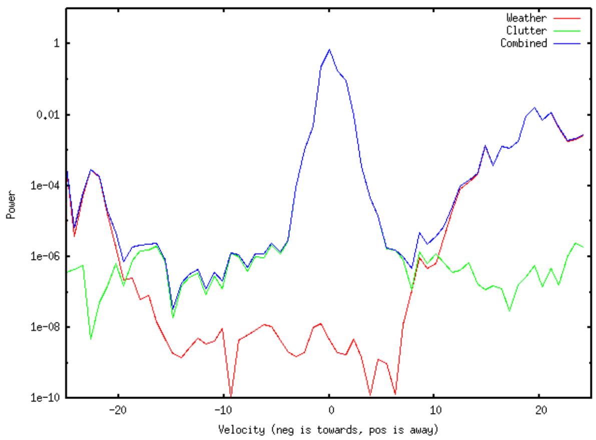

Figure 1: Combined 64-point clutter/weather spectrum.
CSR 20 dB, clutter width 0.5 ms^{-1}.
Weather velocity 20 ms^{-1}, width 2.5 ms^{-1}

In this example, the Nyquist folding velocity is 25 ms^{-1}, such that the right hand axis represents a velocity of 25 ms^{-1} away from the radar and the left hand axis 25 ms^{-1} towards the radar. The weather signal has a velocity of 20 ms^{-1} away from the radar and a spectrum width of 2.5 ms^{-1}. The clutter has a spectrum width of 0.5 ms^{-1} and a clutter-to-weather ratio (CWR) of 20 dB, which means that the clutter power is 100 times as strong as the weather power. (CWR = $10\log_{10}$(clutter power / weather power).)

In the case presented in Figure 1, the clutter peak and the weather peak are separate and distinct. The clutter feature lies at the center of the plot and the weather feature to the right hand side, and they do not overlap significantly. Identifying the clutter and removing it from the weather is reasonably simple. As we shall see later, a sophisticated filter can deal with this type of situation using information from only the combined spectra at a single gate.

Figure 2 shows the same clutter, combined with a weather velocity of 5 ms^{-1} instead of 20 ms^{-1}. There is considerable overlap between the clutter and weather features. Nevertheless, the peaks are still separate. Furthermore, the weather has a wide spectrum while the clutter spectrum is narrow, which means that much of the weather power lies outside the clutter spectrum. Certain filters can do a good job of handling this type of spectrum.

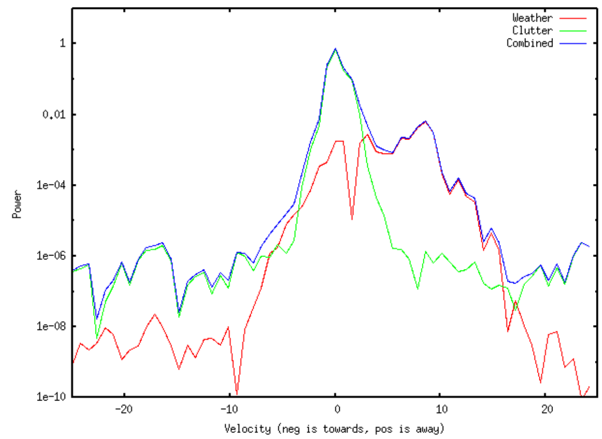

Figure 2: Combined clutter/weather spectrum.
CSR 20 dB, Clutter width 0.5 ms^{-1}.
Weather velocity 5 /ms, width 2.5 ms^{-1}.

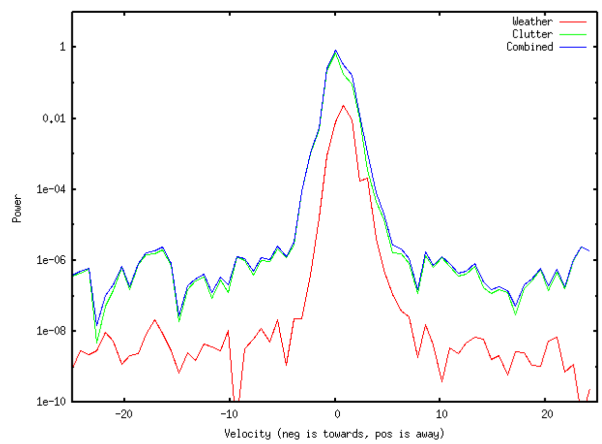

Figure 3: Combined clutter/weather spectrum.
CSR 20 dB, Clutter width 0.5 ms^{-1}.
Weather velocity 1 /ms, width 0.5 ms^{-1}.

Figure 3, on the other hand, shows the same clutter spectrum as in the previous cases, combined with a weather spectrum with a velocity of 1 ms^{-1} – quite close to 0 – and a narrow width of only 0.5 ms^{-1}. For this case, the weather and clutter peaks merge into a singe feature and it is clear that separating the components using only the information in the combined spectrum at a single gate is not possible.

The situation depicted in Figure 3 occurs quite commonly in the case of stratiform precipitation. The precipitation spectrum can be quite narrow, and there will often be regions in the echo with velocities close to zero. Therefore, a comprehensive clutter mitigation strategy is required to handle this situation.

3 Fixed notch clutter filters

Many early clutter filters deployed operationally employed a fixed band width time domain filter (Stanley 1975; Bringi and Chandrasekar 2001). These filters are designed to have a 3 dB bandwidth that would correspond to typical clutter spectral widths. Standardized time domain filters have bandwidths, bandstop and rejection design criteria. In contrast, spectral filters can not only simply “notch out” the desired spectral points but they can also interpolate again across the notched-out region as an estimate for the likely weather signal that might have been eliminated.

Figure 4 shows the result of applying a simple spectral notch filter to the combined clutter and weather spectrum from Figure 2. Typically a notch has a fixed width and depth. As this example shows, there is a tendency for such fixed bandwidth filters to remove more than just the clutter power, since some of the weather power has also been removed.

Fixed bandwidth time domain filters have the advantage of simplicity and speed. The latter was of particular importance in the 1980’s and 1990’s because affordable computers were not fast enough to perform sophisticated spectral processing for each radar gate. Since clutter time domain filters (called Infinite Impulse Response (IIR) filters) operate directly on the I and Q time samples, this was a computationally efficient and practical way to reduce clutter signatures.

The disadvantage of fixed notch width filters is that, when used in isolation and applied everywhere, they often can remove power from the weather echoes. For example these filters will remove valid weather reflectivity from areas of stratiform precipitation with velocities close to 0.

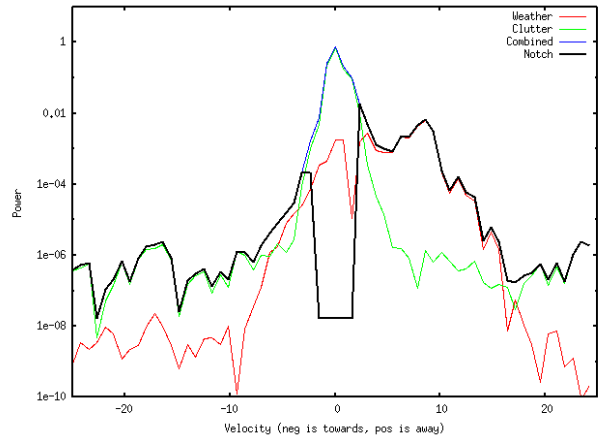

Figure 4: Notch filter applied to combined weather and clutter spectrum.

4 Adaptive clutter filters

As computer costs have decreased and computing power increased, it has become practical to apply more sophisticated spectral-domain clutter filtering on a gate-by-gate basis for scanning radars. These second-generation filters analyze the shape of the spectra and adaptively decide where to reduce the clutter power. The potential of frequency domain filtering has been recognized earlier. (Passarelli et. al., 1981).

Two such adaptive filters are discussed next.

4.1 GMAP filter

The Gaussian Model Adaptive Processing (GMAP) filter was developed by Sigmet, Inc. and is described by Siggia and Passarelli (2004). As indicated by its name, GMAP assumes that the clutter and weather spectra have approximately Gaussian shapes. The spectrum width of the clutter is specified by the user. Given the clutter spectrum width and the power from the central near-zero velocity spectral points, a suitable Gaussian curve is estimated for the clutter. This curve intersects the noise floor at two points. The interval between these two points defines the initial notch for the filter. A Gaussian curve is fitted to the points outside of the notch, which are assumed to represent the weather. The Gaussian curve is then used to estimate the weather power at the points within the initial notch. The Gaussian fit and power estimation steps are then repeated until the power and velocity of the filtered spectrum do not change significantly.

4.2 SSEF filter

GMAP is an effective filter and has been shown to meet the specifications for the WSR-88D (Ice et. al, 2004). However, the implementation (i.e. computer code) is proprietary. Therefore we decided to develop a similar algorithm with a publicly available implementation such that it could be freely used for this study and for research purposes in general.

There are two primary differences between SSEF and GMAP: (a) rather than using a Gaussian model to determine the initial notch, an aggressive notch (typically 1.5 ms^{-1} wide) is used; and (b) logic was added to identify the location of the weather peak. This was done in order to center the final Gaussian fit on the weather peak.

Figures 5, 6 and 7 show the results of applying SSEF to the spectra in Figures 1, 2 and 3. The adaptive filter works well in the first two cases, removing the clutter power while leaving the weather power largely unaffected. In the third case, however, the result is not as good and some of the weather power is removed as well. It is difficult to separate the two spectra that have very similar characteristics. This limitation will be further demonstrated in the next section.

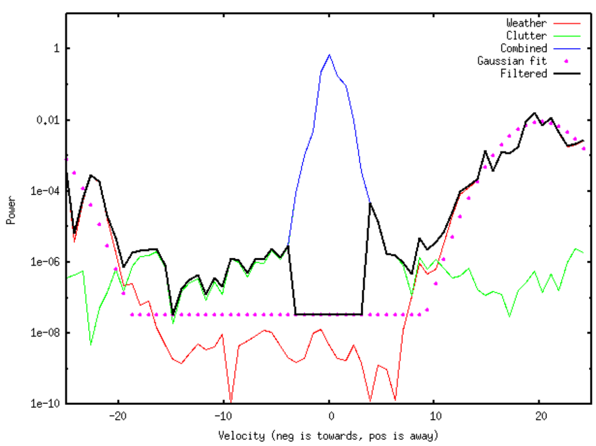

Figure 5: SSEF applied to combined spectrum in Fig. 1.

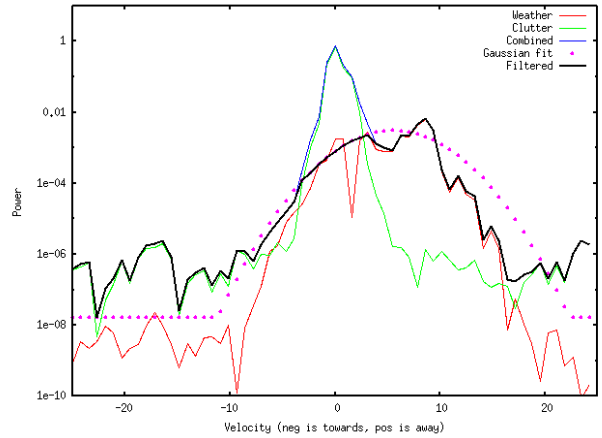

Figure 6: SSEF applied to combined spectrum in Fig. 2.

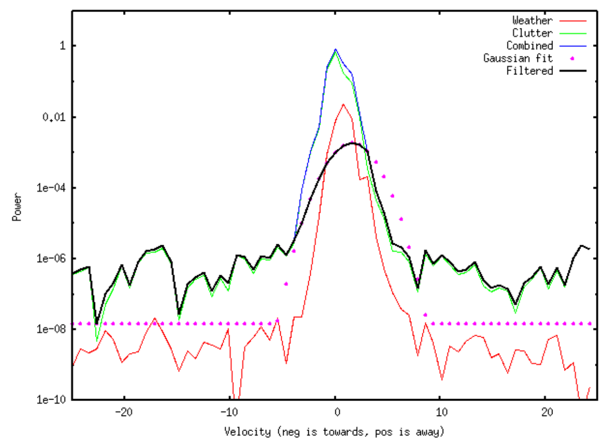

Figure 7: SSEF applied to combined spectrum in Fig 3.

5 Applying an adaptive filter in a situation with stratiform precipitation

Figures 8, 9 and 10 show the unfiltered reflectivity, velocity and spectrum width respectively for a case from the KJIM radar, a WSR-88D test-bed located in Norman, OK. The data were taken at 10:50 UTC on 9 April 2004. A band of stratiform precipitation lies to the W and NW of the radar. Ground clutter exists around the radar and to the south of the radar.

Figure 11 shows the reflectivity after application of the SSEF filter at every gate. Figure 12 shows the clutter power as determined by SSEF.

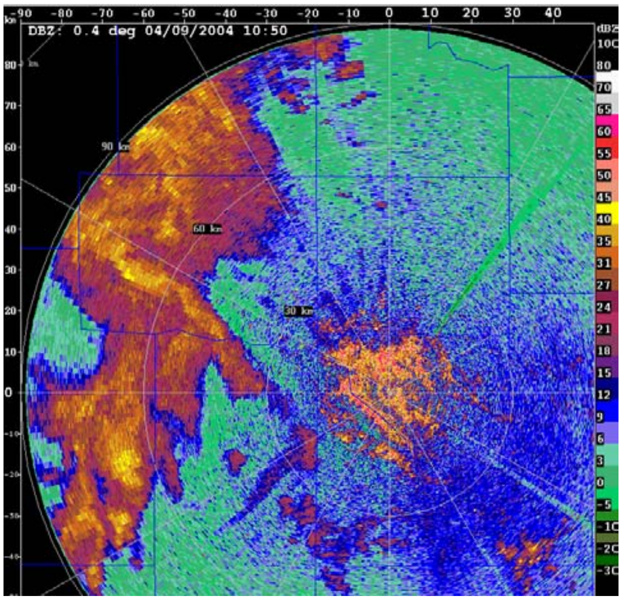

Figure 8: Unfiltered reflectivity – KJIM radar case

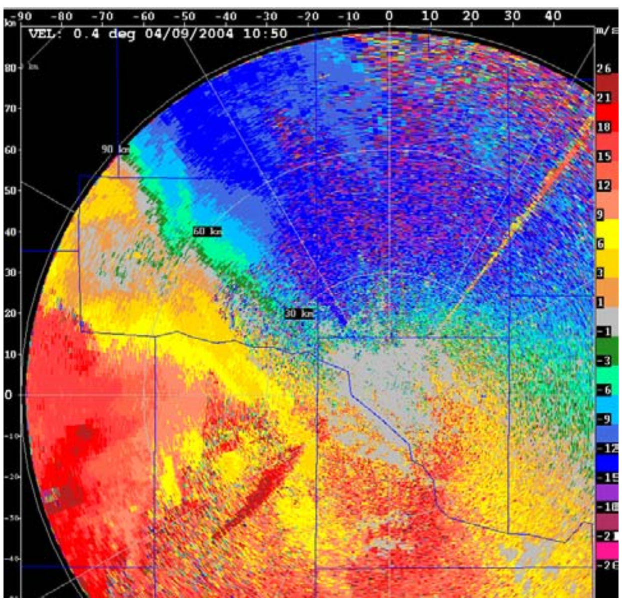

Figure 9: Unfiltered velocity – KJIM radar case

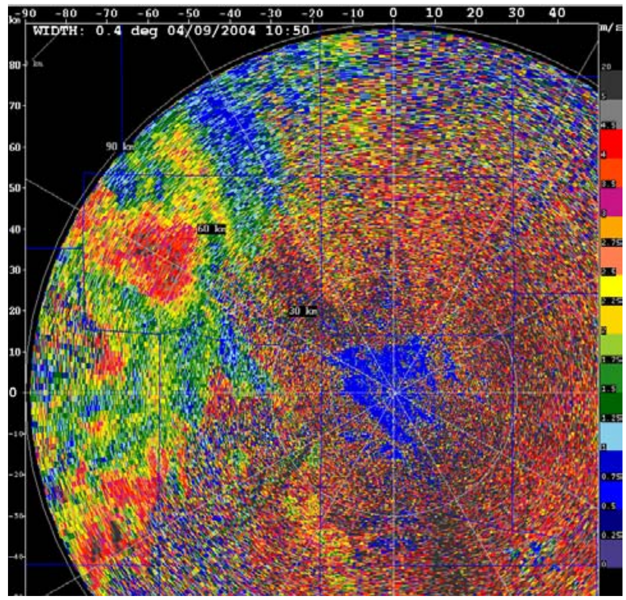

Figure 10: Unfiltered spectrum width – KJIM radar case

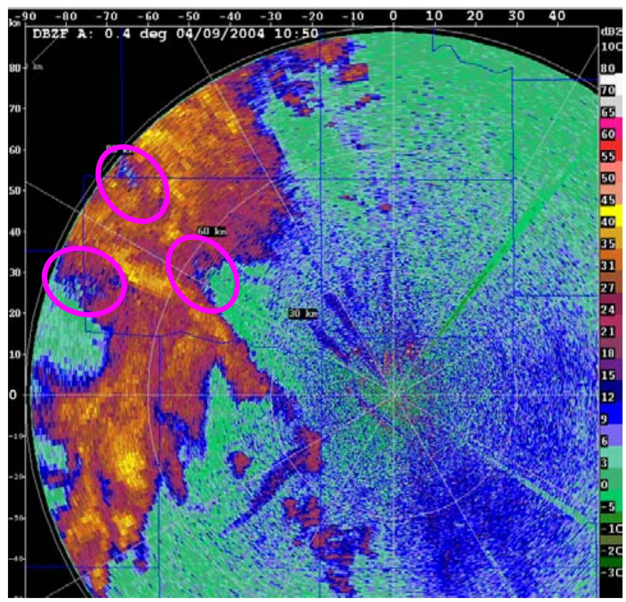

Figure 11: KJIM Reflectivity after application of the SSEF filter at all gates. Magenta ellipses indicate regions where reflectivity was decreased by the filter in error.

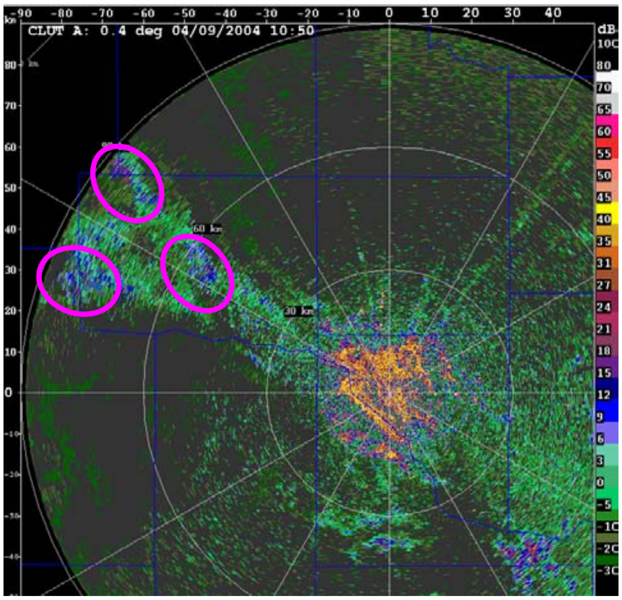

Figure 12: Clutter for KJIM case as computed by applying SSEF at all gates

The filter does a good job of correctly identifying clutter and removing it in most parts of the PPI. However, there are three regions where weather power was removed in error and they are high-lighted by the magenta ellipses. Referring to Figures 9 and 10, it can be seen that these are regions with velocities close to zero and with narrow spectrum widths.

This is precisely the situation mentioned earlier, of stratiform precipitation exhibiting low spectrum widths and velocities close to 0 ms^{-1}. This demonstrates that it is not sufficient to use the clutter filter alone to make decisions about where to remove clutter.

In the next section, we introduce a technique which helps us to make the decision on whether to apply the filter or not.

6 The Clutter Mitigation Decision System (CMDS)

The Radar Echo Classifier (REC) (Kessinger et. al, 2003) is a software tool designed to classify radar echoes into categories such as ground clutter, sea clutter, and precipitation.

In this study, we developed a decision system, using similar fuzzy logic techniques, to identify ground clutter and anomalous propagation (AP) returns. The Clutter Mitigation Decision System (CMDS) is designed to identify echo regions that are likely to contain clutter, such that the clutter filter is applied only to those regions. The problem of removing power from weather echoes is thereby avoided.

The desirable properties of the CMDS are that:

- It must be sufficiently fast and efficient to operate in real-time within the WSR-88D Open Radar Data Acquisition (ORDA).
- It must accept time series data, such that the algorithm can perform spectral processing, if required.
- It should be able to detect both AP and NP ground clutter.

The CMDS computes echo properties based on values not only from the gate of interest but from surrounding gates as well. NEXRAD data were used for this study, with an azimuthal spacing of 1 degree and 250 m gate spacing. The CMDS was set up to use a computational 'kernel' 2 km long in range (i.e. 8 gates) and 5 degrees wide in azimuth.

The following feature fields were used in the classifier:

- TDBZ - DBZ texture: squared change in dBZ from one gate to the next, in range, averaged over the kernel.
- SPIN - DBZ 'spin': a measure of how frequently the trend in reflectivity along a beam changes with range. Averaged over the kernel. (Steiner and Smith, 2002).
- VEL: velocity at the gate.
- SDVE: standard deviation of velocity over the kernel.
- WIDTH: spectrum width at the gate.

The CMDS computes each of these fields, and then converts the field value into an *interest value* between 0 and 1 using a so-called membership transfer function. The membership functions used are shown in Figure 13 and Figure 14. The interest values from all fields are combined into a weighted mean, which is a measure of clutter probability. Gates with a

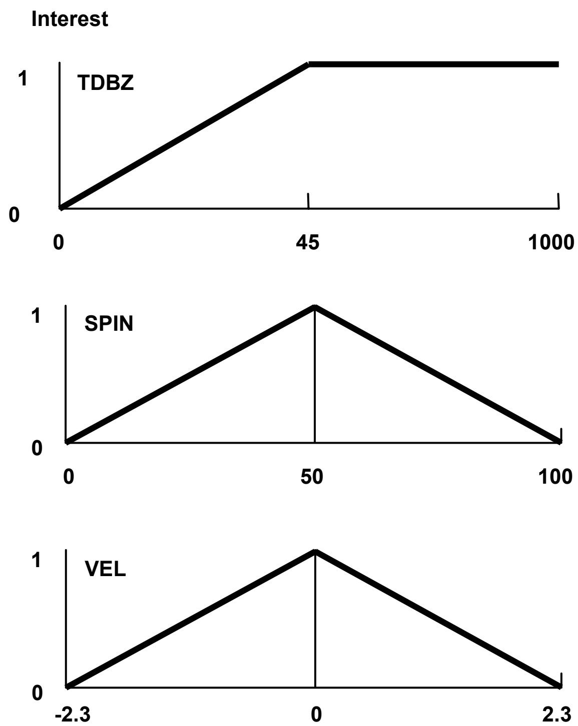

Figure 13: Membership functions for TDBZ, SPIN and VELOCITY

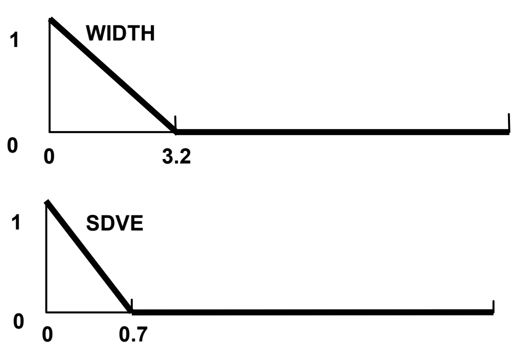

Figure 14: Membership functions for spectrum width and standard deviation of velocity.

clutter probability exceeding 0.5 are considered likely clutter points.

7 Beam processing sequence

Because the CMDS uses data from 2 adjacent beams on either side, for real-time operations a beam queue of 5 beams was set up as shown in Figure 15. The interest fields are computed for the center beam.

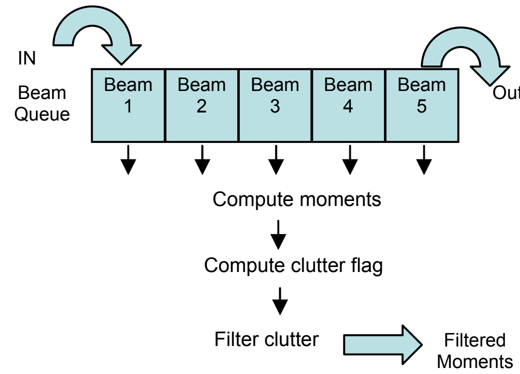

Figure 15: Beam queue processing required to run the CMDS in real-time using time-series data

8 Example of using the CMD system to identify clutter

Figures 16 through 18 show the TDBZ, SPIN and SDVE for this case.

The membership functions are applied to these fields, as well as to velocity and spectrum width and a normalized weighted sum is computed (Figure 19).

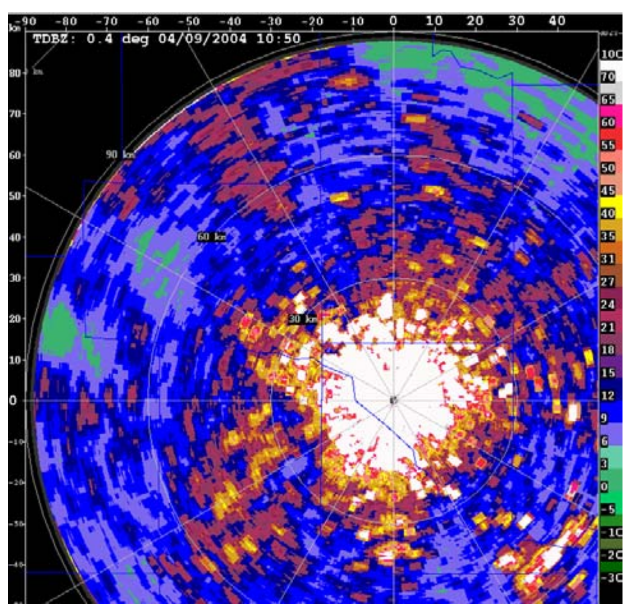

Figure 16: DBZ Texture – KJIM case

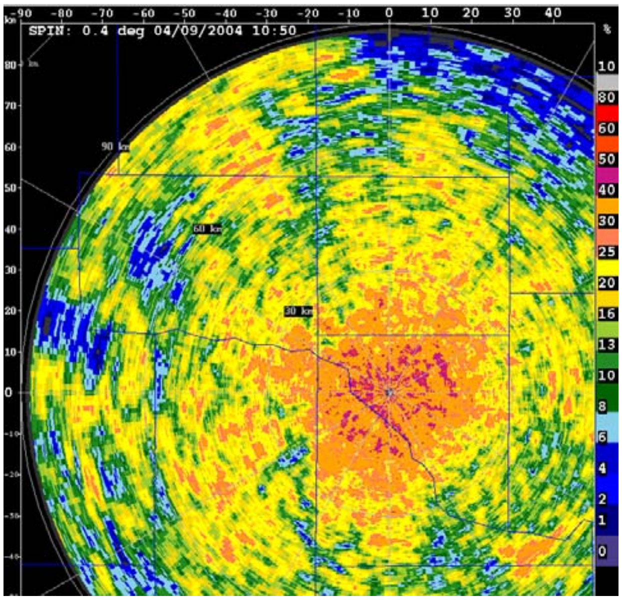

Figure 17: SPIN – KJIM case

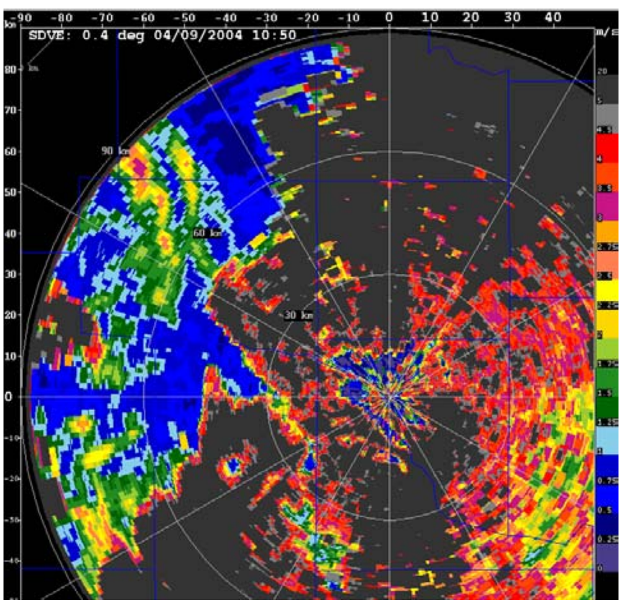

Figure 18: Standard deviation of velocity – KJIM case

Figure 20 shows the final clutter decision flag, which is determined by applying a threshold (in this case 0.5) to the normalized CMDS value (shown in Figure 20). The shaded yellow gates in Figure 20 are those at which clutter is regarded as likely according to the CMDS.

Figures 21, 22 and 23 show the result of applying the clutter filter at only those gates flagged as clutter by the CMDS. The problem

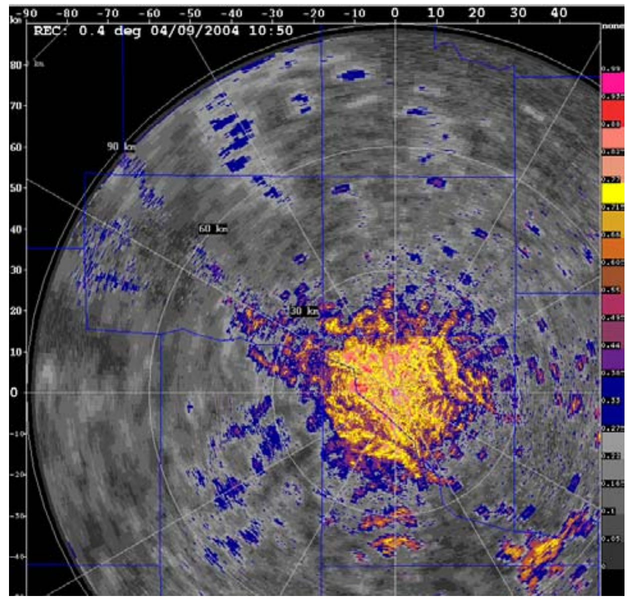

Figure 19: Normalized CMDS – KJIM

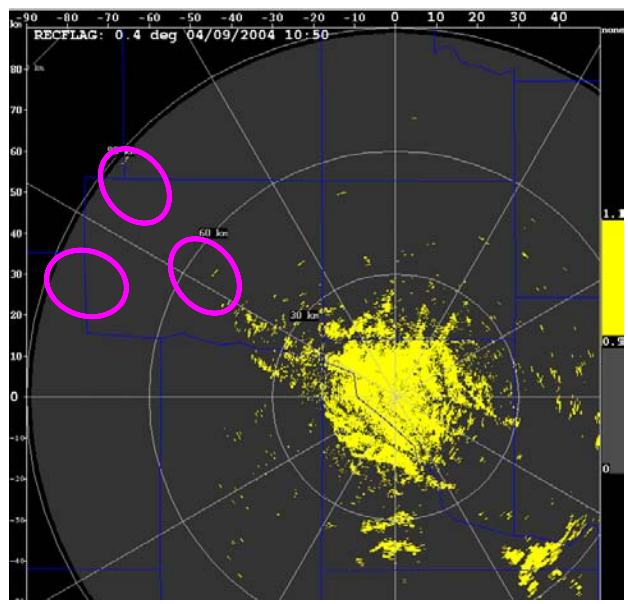

Figure 20: CMDS clutter flag – KJIM

areas that were identified in Figure 12 are no longer an issue because those areas were not identified as having clutter and the filter was not applied in those regions. This is a much improved result and demonstrates the effectiveness of combining the CMDS with an adaptive spectral filter for effective clutter mitigation.

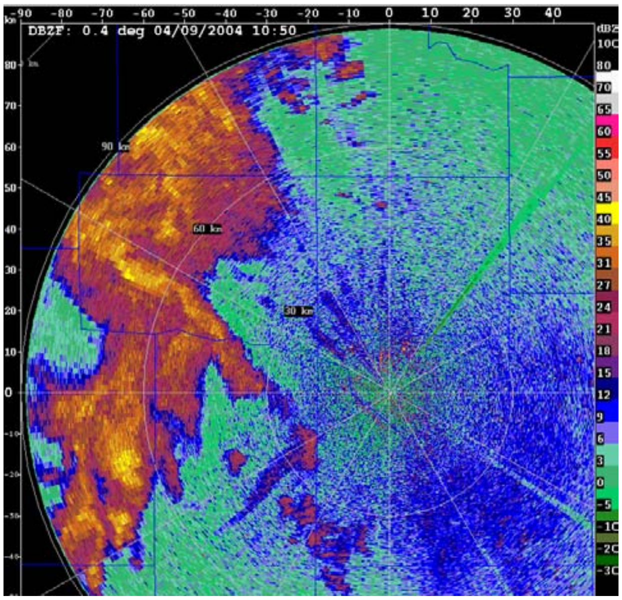

Figure 21: KJIM reflectivity after clutter filtering based on the CMDS clutter flag.

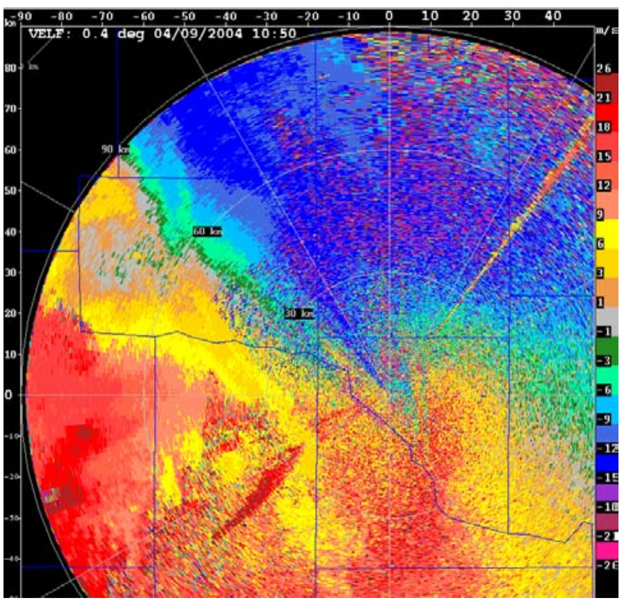

Figure 22: KJIM velocity after filtering based on the CMDS clutter flag.

9 Using dual polarization data for identifying clutter

Dual-polarization fields, if available, are a useful additional source of information for the identification of clutter. In particular the RHOHV field and the spatial variability of ZDR and RHOHV, are good indicators of the

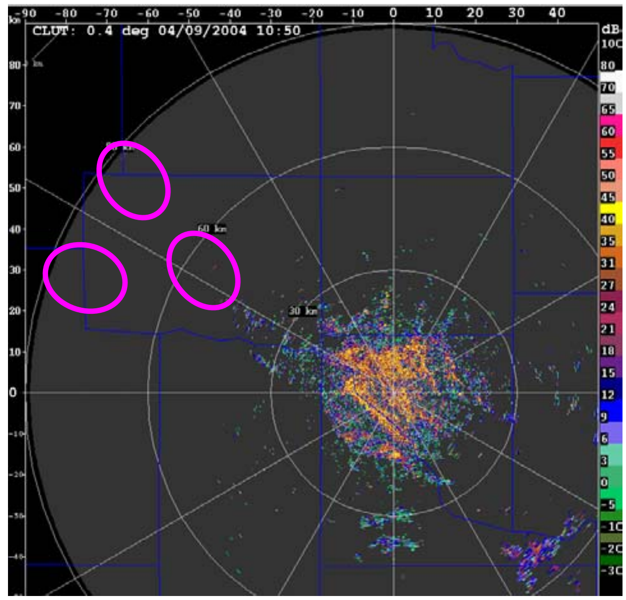

Figure 23: Clutter for KJIM case as computed by applying SSEF at gates flagged for clutter in Figure 20. This should be compared to Figure 12. The magenta ovals from Figure 12 are included to emphasize that the CMDS will not apply the clutter filter within the precipitation.

likelihood of weather as opposed to clutter (Vivekanandan et. al., 1999). In the case of ZDR and RHOHV, the spatial variability is computed in range only, rather than over the range/azimuth kernel. The advantage of this technique is that it eliminates the smearing in azimuth which is apparent in the TDBZ and SPIN fields.

The above three dual-polarization fields were tested in the CMDS using data from the NCAR SPOL radar collected in Mexico during the North American Monsoon Experiment (NAME) field campaign conducted in the summer of 2004. The membership functions applied for each of these three fields are shown in Figure 24.

Figure 25 shows the normalized CMDS field without the dual polarization fields while Figure 26 shows the result with the dual-polarization fields included. (The concentric rings near the maximum radar range are produced by a test pulse and should be ignored.)

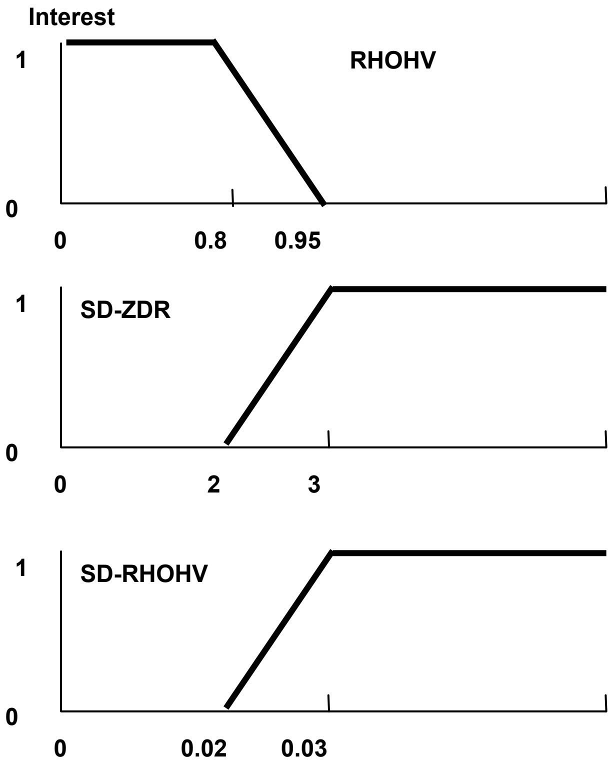

Figure 24: Membership functions for dual polarization variables.

The two fields are similar, indicating that the information contained in the various CMDS fields is complementary. The advantages of including the dual polarization fields are that (a) the dual polarization fields are an independent measure of clutter likelihood, and therefore improve the confidence of the result and (b) because the dual polarization statistics are applied in range only, rather than across adjacent azimuths, the smearing in azimuth evident in Figure 25 is somewhat reduced.

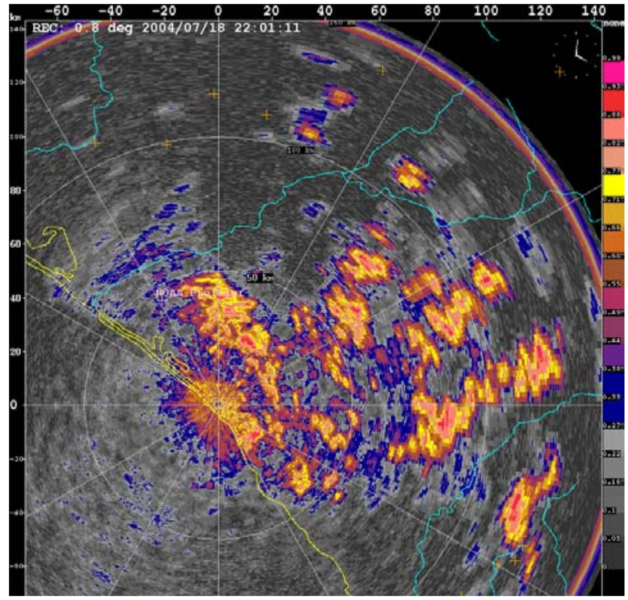

Figure 25: Normalized CMDS field, without dual-polarization fields

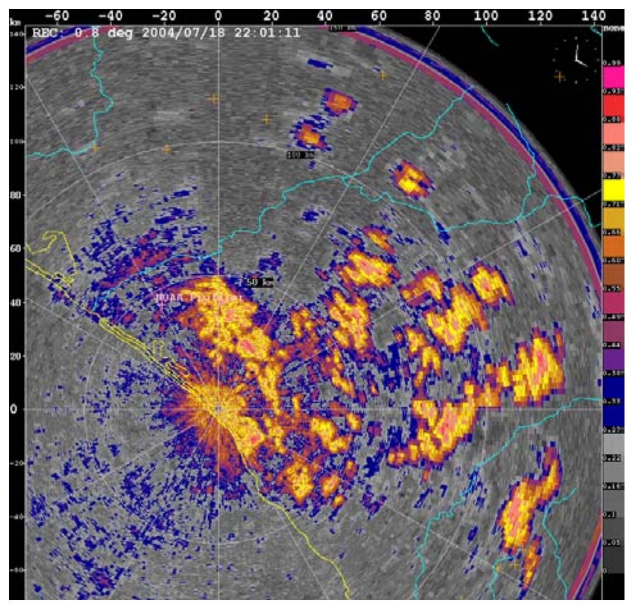

Figure 26: Normalized CMDS field, including dual-polarization fields

10 Conclusions

The application of adaptive spectral clutter filters leads to a marked improvement over IIR time domain filters in terms of preserving weather power. However, errors still occur when the weather spectrum has a narrow width and a velocity close to zero. The Clutter Mitigation Decision System is a useful additional tool to identify regions with clutter and therefore to limit the application of the clutter filters to those areas most likely to have clutter. This minimizes the probability that weather power will be incorrectly removed by the clutter filter.

11 Future work

Further work is needed to confirm the skill of dual polarization fields in separating weather from clutter. However, all indications are that this is a sound technique. In addition, early work in using pattern recognition to assess clutter probability by analyzing spectra at successive range gates shows promise for improving the performance of the CMDS.

Acknowledgements

NCAR is sponsored by the National Science Foundation. This research is funded by the National Oceanic and Atmospheric Administration (NOAA) Radar Operations Center (ROC), Norman, OK.

References

Ice, R. L., R. D. Rhoton, D. S. Saxion, N. K. Patel, S. Sirmans, D. A. Warde, D. L. Rachel and R. G. Fehlen, 2004: ROC Evaluation of the WSR-88D ORDA System Signal Processing. *Preprints-CD, 20th International Conference on Interactive Information Processing Systems for Meteorology, Oceanography and Hydrology*.

Kessinger, C. et. al., 2003: The radar echo classifier: a fuzzy logic algorithm for the WSR-88D. *Preprints, 3rd Conference on Artificial Intelligence Applications to the Environmental Science*, AMS, 9-13 February 2003, Long Beach, CA

Siggia, A., D. and R. Passarelli Jr., 2004: Gaussian model adaptive processing (GMAP) for improved ground clutter cancellation and moment calculation. *Proceedings, Third European Conference on Radar in Meteorology and Hydrology (ERAD)*:67-73.

Steiner, M., and J.A. Smith, 2002: Use of three-dimensional reflectivity structure for automated detection and removal of non-precipitating echoes in radar data. *Journal of Atmospheric and Oceanic Technology*, **19** (5), pp. 673-686.

Bringi, V. N. and V. Chandrasekar, 2001: *Polarimetric Doppler Weather Radar, Principles and applications*. Cambridge University Press.

Vivekanandan, J., D.S. Zrnic, S. M. Ellis, R. Oye, A.V. Ryzhkov, and J. Straka, 1999: Cloud microphysics retrieval using S-band dual-polarization radar measurements. *Bulletin of the American Meteorological Society,* **80,** 381-388.

Passarelli et. al., 1981: Ground Clutter Rejection in the Frequency Domain. *Preprints, 20th Conference on Radar Meteorology*, AMS, Boston.

Stanley, W. D., 1975: *Digital Signal Processing*. Reston Publishing.